

Center for Quality and Applied Statistics
Kate Gleason College of Engineering
Rochester Institute of Technology

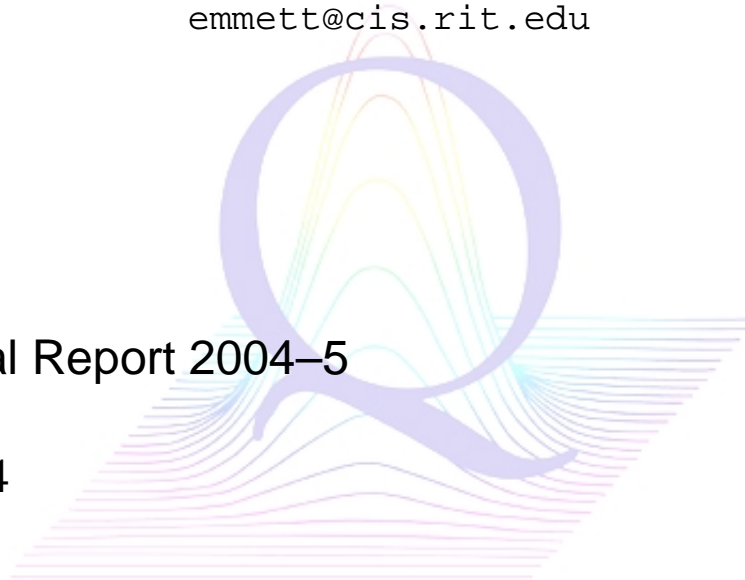
**Geometric Basis-Vector Selection Methods
and Subpixel Target Detection as Applied to
Hyperspectral Imagery**

Peter Bajorski
Center for Quality and Applied Statistics
Rochester Institute of Technology
pxbeqa@rit.edu

Emmett J. Ientilucci
Chester F. Carlson Center for Imaging Science
Rochester Institute of Technology
emmett@cis.rit.edu

Technical Report 2004-5

June 2004



Geometric Basis-Vector Selection Methods and Subpixel Target Detection as Applied to Hyperspectral Imagery

Peter Bajorski

Center for Quality and Applied Statistics
Graduate Statistics Department
Rochester Institute of Technology
Rochester, NY, USA
Email: Peter.Bajorski@rit.edu

Emmett J. Ientilucci

Digital Imaging and Remote Sensing Laboratory
Chester F. Carlson Center for Imaging Science
Rochester Institute of Technology
Rochester, NY, USA
Email: emmett@cis.rit.edu

Abstract—In this paper, we compare three basis-vector selection methods as applied to subpixel target detection. This is a continuation of previous research in which a similar comparison was performed based on an AVIRIS image. Our goal is to find out to what extent our previous observations apply more broadly to other images, more specifically, a HYDICE image used in this paper. Our target detection approach is based on generating a radiance target region using a physical model to generate radiance spectra as observed under a wide range of atmospheric, illumination, and viewing conditions. The advantage of this approach is that the resulting target detection is invariant to those changing conditions. For the purpose of target detection, we use a structured model to describe each image spectra as a linear combination of the target and background basis-vectors, and then we apply a matched subspace detector. Finally, we find ROC curves to describe the relationship between the detection rate (DR) and the false alarm rate (FAR). Due to a large number of cases considered, we use summary metrics to represent our results. The obtained results are quite different from those obtained in [1] for the AVIRIS image. The best method for generating the background basis vectors in the AVIRIS image was the MaxD method, while the SVD method proved to be best for the HYDICE image used in this paper. Further research is needed to find out the reasons for these differences. It is not surprising that different methods are optimal for different types of data. However, it would be useful to be able to recognize the optimal method without assuming knowledge of the targets in the image.

Keywords- *Hyperspectral, Subpixel Target Detection, Endmember, Basis Vector, HYDICE*

I. INTRODUCTION

In [1], three basis-vector selection methods were compared as applied to subpixel target detection. The goal of this paper is to perform a similar comparison on a different (HYDICE) image in order to find out to what extent the observations made in [1] apply more broadly to other images.

Our premise is that we know what the target is and can characterize it in terms of its reflectance spectrum. Furthermore, we assume the target may exist at spatial scales

such that it will present itself as a fraction of a pixel, and that it may exist in a significant number of pixels (more specifically, we cannot assume that a significant region of the image does not contain any targets). We desire a data processing approach that can mitigate atmospheric and illumination effects such that atmospheric correction is not a required prerequisite for the method. The approach presented here involves defining a radiance target region that consists of all target spectra that can be observed under a wide range of atmospheric, illumination, and viewing conditions that might exist in the scene. In practice, a finite number of spectra (448 in our case) is generated using the MODTRAN radiation propagation model. A convex hull spanned by those spectra in a p -dimensional space (where p is the number of spectral bands) is defined as the radiance target region. The idea is that the radiance target region should include other spectra that might be observed under some other atmospheric, illumination, and viewing conditions that were not taken into account during the MODTRAN generation process. In other words, if a pure target were observed in the image, it would manifest itself somewhere within the radiance target region, and it would not be expected outside of that region. The advantage of the radiance target region is that it can be used for target detection in images created under any atmospheric, illumination, and viewing conditions. More on this invariant approach and the physics-based model can be found in [1] and [2].

In this paper, we characterize the target and background regions using endmembers generated by three different methods—the pixel purity index (PPI), the singular value decomposition (SVD), and the maximum distance (MaxD). All three methods and the related literature are discussed in [1].

The target and background endmembers are used in a structured model that attempts to describe all image spectra. Based on this model, we construct a matched subspace detector and investigate the resulting false alarm rates.

II. TARGET DETECTION IN STRUCTURED MODELS

For the purpose of sub-pixel target detection, we use a geometric approach that leads to structured models. For an

overview of target detection approaches and their classification, see [3] and [4].

Let us consider an image consisting of N pixels. Each pixel is represented by a p -dimensional vector of spectrum \mathbf{x}_i , where p is the number of spectral bands, and $i=1, \dots, N$. We are assuming the following structured model:

$$\mathbf{x}_i = \mathbf{T} \cdot \mathbf{a}_i + \mathbf{B} \cdot \mathbf{b}_i + \boldsymbol{\varepsilon}_i \quad (1)$$

where \mathbf{T} is a fixed matrix of the target basis vectors, \mathbf{B} is a fixed matrix of background basis vectors, and \mathbf{a}_i , \mathbf{b}_i are unknown vectors. The vector $\boldsymbol{\varepsilon}_i$ represents approximation errors, which can be due to the noise in data or a modeling error (or both).

The target detection problem can be defined as the hypothesis-testing problem for testing the null hypothesis that all values in the vector \mathbf{a}_i are zero, that is,

$$H_0 : \mathbf{a}_i = \mathbf{0}$$

where $\mathbf{0}$ is a vector of zeros, versus the alternative hypothesis

$$H_1 : \mathbf{a}_i \neq \mathbf{0}$$

Due to physical constraints, the coordinates of the vector \mathbf{a}_i could be required to be positive (or even sum up to 1), but such constraints are not explicitly needed in the detection methods used in this paper.

All target detection in this paper is done for a matched subspace detector (MSD):

$$MSD(\mathbf{x}) = \frac{\mathbf{x}^T (\mathbf{P}_Z - \mathbf{P}_B) \mathbf{x}}{\mathbf{x}^T (\mathbf{I} - \mathbf{P}_Z) \mathbf{x}}$$

where \mathbf{I} is the identity matrix, $\mathbf{Z} = [\mathbf{T} \ \mathbf{B}]$ is a matrix consisting of all columns of \mathbf{T} and \mathbf{B} , and \mathbf{P}_Y (for \mathbf{Y} equal to \mathbf{B} or \mathbf{Z}) is the matrix of the projection onto the space generated by columns of \mathbf{Y} , that is,

$$\mathbf{P}_Y = \mathbf{Y}(\mathbf{Y}^T \mathbf{Y})^{-1} \mathbf{Y}^T.$$

Under certain assumptions (see [1]), the MSD detector is equivalent to the Generalized Likelihood Ratio test statistic for testing H_0 versus H_1 .

III. METRICS FOR EVALUATION OF TARGET DETECTION METHODS

We evaluate performance of the basis vector selection techniques based on the observed ROC curves. An observed ROC curve is a plot of detection rate (DR) versus false alarm rate (FAR). We specifically use the term ‘‘detection rate’’ rather than ‘‘probability of detection’’ because these results are based on the observed frequency of detecting the target rather than on theoretical calculations of probabilities.

Due to a large number of cases considered, it would not be effective to simply plot the observed ROC curves (2160 curves would be needed). Hence, some summary metrics were required. In addition to summarizing detection rates (DR) at several FAR levels, we also used a new summary metric called an Average FAR (AFAR). In order to define AFAR, let us assume that there are k pixels in the image that contain the target. The observed ROC curve is fully described by k numbers $r_i, i=1, \dots, k$, where r_i is the lowest FAR to achieve i/k detection rate (DR). The AFAR is defined as

$$AFAR = \frac{1}{k} \sum_{i=1}^k r_i$$

If the observed ROC curve is plotted as a step function

$$ROC(x) = \min\{i/k : r_i \leq x\}, \text{ for } 0 \leq x \leq 1,$$

then AFAR is the area above the observed ROC curve (to be more precise, the area between the observed ROC curve and the DR level of 1). Consequently, AFAR can also be expressed as one minus the area under the observed ROC curve. These and some other performance metrics are described in [1].

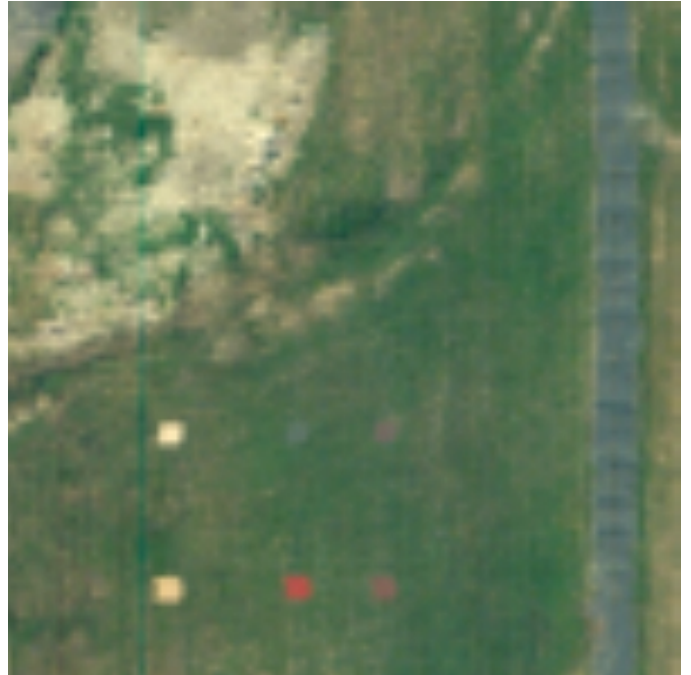


Figure 1. 100 x 100 pixel HYDICE image showing a series of target panels (at the bottom of the image), one of which was used in this paper. The target of interest was made up of 8 fully resolved pixels and 4 mixed or sub-pixels.

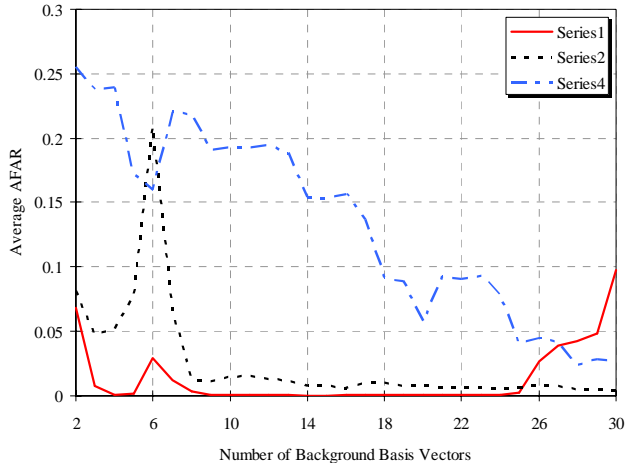


Figure 2. Average AFAR results when using the SVD method for obtaining target basis-vectors as applied to the target regions and the three investigated methods (SVD, MaxD, and PPI) used for the background region.

IV. RESULTS

In this section, we present numerical results on comparisons of the three basis vector selection techniques (SVD, MaxD, and PPI). Specifically, we use each of the three techniques for generating both the target and background basis vectors. This creates a total of 9 combinations. For each of the 9 combinations, we identify up to 8 target basis vectors and up to 30 background basis vectors. This gives a matrix of $8 \cdot 30 = 240$ combinations (by taking the first $i = 1, \dots, 8$ target basis vectors and the first $j = 1, \dots, 20$ background basis vectors). If we wanted the observed ROC curves for all of these cases, we would need $9 \cdot 240 = 2,160$ curves—thus, the motivation to develop the metrics outlined in Section III.

The dataset used for the analysis can be seen in Figure 1. Here we have a 100×100 pixel subsection from a larger HYDICE image. After the removal of water bands, we are left with a total of 170 valid spectral bands. The target of interest contains 8 fully resolved pixels and 4 sub-pixels for a total of 12 target pixels. These target pixels were chosen using previously developed truth masks.

Since we identify 12 pixels as containing our target spectrum, it means that $k = 12$ in the notation of Section III. For each of the 2,160 cases, we calculate the 12 FAR values $r_i, i = 1, \dots, 12$. The resulting AFAR and detection rates are discussed in the following two subsections.

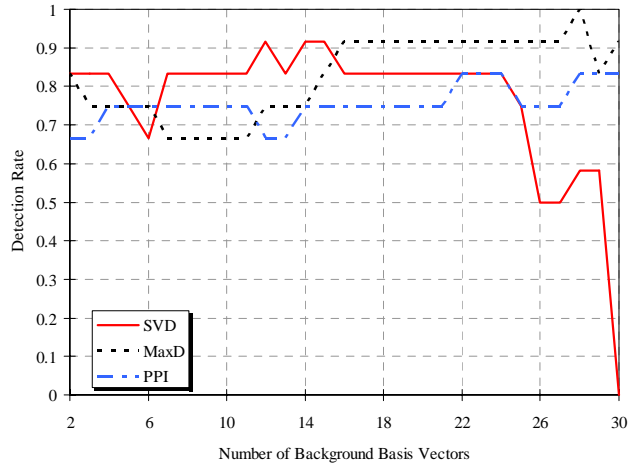


Figure 3. Detection rates for the three methods used as the background basis-vector selection technique when only one SVD target basis vector is utilized.

A. Average False Alarm Rates (AFAR)

We observed that the AFAR values were not strongly influenced by the number of target basis vectors (except that results for one target basis vector were somewhat lower). Consequently, we calculated the average AFAR values over the range between 2 and 8 target basis vectors and plotted the results for all 9 combinations of the three basis-vector selection techniques. It turned out that the results were not influenced by the basis-vector selection techniques applied to the target regions. Figure 2 shows those results plotted using SVD as the method of selecting basis-vectors, as applied to the target region and the three investigated methods (SVD, MaxD, and PPI) used for the background region.

B. Detection Rates

In this section, we fix the acceptable level of false alarm rate to 10^{-4} , and analyze the resulting detection rates. That is, we show what fraction of targets is detected if only 1 false alarm in 10,000 pixels is acceptable. Contrary to the AFAR results, the detection rates strongly depend on the number of target basis vectors used. The results also depend on the method used for the generation of the target basis vectors. Overall, the SVD method is most efficient as the target basis-vector selection technique. Figure 3 shows detection rates for the three methods used as the background basis-vector selection techniques, when only one SVD target basis vector is utilized. All three methods show similar performance in the range between 2 and 25 background basis vectors. Very similar properties were observed when two SVD target basis vectors were used.

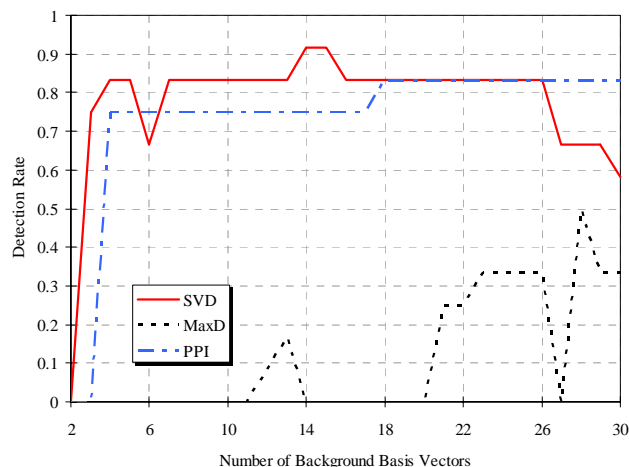


Figure 4. Detection rates for the three methods used as the background basis-vector selection technique when three SVD target basis vectors are utilized.

On the other hand, for three or more SVD target basis vectors used, the performance of MaxD used as the background method was much below that of the two remaining methods (see Figure 4).

V. CONCLUSIONS

The purpose of this study was to find out to what extent the observations made in our previous study [1] apply to a HYDICE image, and possibly more broadly to other images. We conclude that the results for the HYDICE image are substantially different from those for the AVIRIS image used in [1]. For example, SVD turned out to be the best (of the three) method for generating the background basis vectors, which means a much better performance than that observed for the AVIRIS image. Another difference is the strong dependence on the number of target basis vectors and the method used to generate them.

When trying to detect our specific target in the HYDICE image, the best method seems to be SVD applied to obtain both the target and background basis vectors. The number of recommended basis vectors is one basis vector for describing the target region and between 9 and 25 basis vectors (although 2 basis vectors also work quite well) for describing the background region.

Overall, perhaps this difference is not that surprising since the composition of the two data sets was completely different. The sample region obtained in the AVIRIS image contained an order of magnitude more materials (or classes) than was seen in the HYDICE image. This overall difference in spatial and spectral complexity could be the source of our differences. Further research is needed to determine the reasons for those differences. However, it would be useful to be able to recognize the optimal method without assuming knowledge of the targets.

REFERENCES

- [1] P. Bajorski, E. Ientilucci, and J. Schott. "Comparison of Basis-Vector Selection Methods for Target and Background Subspaces as Applied to Subpixel Target Detection" (to appear in Proc. SPIE, Algorithms and Technologies for Multispectral, Hyperspectral, and Ultraspectral Imagery X, , Orlando, FL, April 2004).
- [2] G. Healey and D. Slater. Models and methods for automated material identification in hyperspectral imagery acquired under unknown illumination and atmospheric conditions. *IEEE Transactions on Geoscience and Remote Sensing*, 37 (6), pp. 2706-2717, November 1999.
- [3] D. Manolakis. Overview of algorithms for hyperspectral target detection: theory and practice. In Proc. SPIE Algorithms and Technologies for Multispectral, Hyperspectral, and Ultraspectral Imagery VIII, volume 4725, pp. 202-251, Orlando, FL, April 2002.
- [4] D. Manolakis and G. Shaw. Detection algorithms for hyperspectral imaging applications. *IEEE Signal Processing Magazine*, 19 (1):29-43, January 2002.